Paleobiology

cambridge.org/pab

Oxygen isotope composition of teeth suggests endothermy and possible migration in some Late Cretaceous shark taxa from the Gulf Coastal Plain, USA

Chelsea M. Comans[1], Thomas S. Tobin[1,2] and Rebecca L. Totten[1,2]

[1]Department of Geological Sciences, University of Alabama, Tuscaloosa, Alabama 35487, U.S.A.
[2]Alabama Museum of Natural History, Tuscaloosa, Alabama 35487, U.S.A.

Article

Cite this article: Comans CM, Tobin TS, Totten RL (2025). Oxygen isotope composition of teeth suggests endothermy and possible migration in some Late Cretaceous shark taxa from the Gulf Coastal Plain, USA. *Paleobiology* 1–13. https://doi.org/10.1017/pab.2024.45

Received: 7 February 2024
Revised: 21 August 2024
Accepted: 6 September 2024

Corresponding author:
Chelsea M. Comans;
Email: cmcomans@crimson.ua.edu

PALEOBIOLOGY A PUBLICATION OF THE Paleontological SOCIETY

CAMBRIDGE UNIVERSITY PRESS

Non-technical Summary

Sharks today live in a variety of habitats, but the range of environments occupied by extinct sharks is not well known. The water temperature and chemistry of marine environments is incorporated in the composition of fish teeth, as well as the way organisms regulate their body temperature. To better understand the ecology of ancient sharks, we analyzed the chemical composition (stable oxygen isotope values) of six Late Cretaceous–age (86–79 million years ago) shark species from the Gulf Coastal Plain of Alabama, USA. We also analyzed teeth from the fish *Enchodus petrosus*, which should record ambient water temperature and chemistry, and compared the shark data with that of *E. petrosus*. Two of the shark taxa (*Ptychodus mortoni* and *Cretoxyrhina mantelli*) have much lower values compared with other fossil sharks and the fish *E. petrosus*. The low *P. mortoni* values are best explained by *P. mortoni* having a higher body temperature than the surrounding water, either through active or passive body heating. Similarly, the low *C. mantelli* values are best explained by both migration and higher body temperatures. It was proposed from other evidence that *C. mantelli* had higher body temperatures, but this study marks the first quantitative evidence of higher body temperatures in *P. mortoni*. If *P. mortoni* had an elevated body temperature, then it is likely that body temperature regulation evolved many times in sharks in the geologic past, as this species is not closely related to other species in which this phenomenon is documented.

Abstract

We analyzed the oxygen isotope composition of biogenic apatite phosphate ($\delta^{18}O_p$) in fossil tooth enameloid to investigate the paleoecology of Late Cretaceous sharks in the Gulf Coastal Plain of Alabama, USA. We analyzed six different shark taxa from both the Mooreville Chalk and the Blufftown Formation. We compared shark $\delta^{18}O_p$ with the $\delta^{18}O_p$ of a co-occurring poikilothermic bony fish *Enchodus petrosus* as a reference for ambient conditions. *Enchodus petrosus* tooth enamel $\delta^{18}O_p$ values are similar between formations (21.3‰ and 21.4‰ Vienna Standard Mean Ocean Water [VSMOW], respectively), suggesting minimal differences in water $\delta^{18}O$ between formations. Most shark taxa in this study are characterized by $\delta^{18}O_p$ values that overlap with *E. petrosus* values, indicating they likely lived in similar habitats and were also poikilothermic. *Ptychodus mortoni* and *Cretoxyrhina mantelli* exhibit significantly lower $\delta^{18}O_p$ values than co-occurring *E. petrosus* (*P. mortoni* $\delta^{18}O_p$ is 19.1‰ VSMOW in the Mooreville Chalk; *C mantelli* $\delta^{18}O_p$ is 20.2‰ VSMOW in the Mooreville Chalk and 18.1‰ VSMOW in the Blufftown Formation). Excursions into brackish or freshwater habitats and thermal water-depth gradients are unlikely explanations for the lower *P. mortoni* and *C. mantelli* $\delta^{18}O_p$ values. The low *P. mortoni* $\delta^{18}O_p$ value is best explained by higher body temperature relative to surrounding temperatures due to active heating (e.g., mesothermy) or passive heating due to its large body size (e.g., gigantothermy). The low *C. mantelli* $\delta^{18}O_p$ values are best explained by a combination of mesothermy (e.g., active heating) and migration (e.g., from the Western Interior Seaway, low-latitude warmer waters, or the paleo–Gulf Stream), supporting the hypothesis that mesothermy evolved in lamniform shark taxa during the Late Cretaceous. If the anomalous *P. mortoni* $\delta^{18}O_p$ values are also driven by active thermoregulation, this suggests that mesothermy evolved independently in multiple families of Late Cretaceous sharks.

Introduction

Sharks are cosmopolitan apex predators of both modern and ancient aquatic ecosystems. The evolutionary success of sharks is due in large part to their adaptation to a variety of different habitats, including marine and nonmarine environments. Habitats of extinct shark taxa are

usually assessed through the interpretation of depositional environments from the sedimentary units in which they are found (e.g., Case and Schwimmer 1988; Shimada 2007; Bice and Shimada 2016) and through comparisons with extant analogues (e.g., Welton and Farish 1993; Schwimmer et al. 1997; Shimada 1997b). However, these habitat interpretations based on depositional environments do not consider differences in preferred water column position, time spent in a habitat, or postmortem transport and mixing of remains. Furthermore, sharks continuously shed teeth throughout their lifetimes, and many sharks are migratory, losing teeth in different locations during their life spans. Differential preservation potential across environments (i.e., differences in the conditions at the time and place of burial that allow for preservation) also leads to gaps in our full understanding of biogeographic ranges. Habitat information from extant sharks can help fill some of these gaps, but modern taxa are limited in their usefulness as analogues due to significant differences in climate and ecosystem structure.

Stable oxygen isotope analysis of biogenic apatite phosphate ($\delta^{18}O_p$) in shark tooth enameloid has the potential to be an additional, more precise paleohabitat proxy. Shark teeth consist of an internal, porous dentin layer and an outer, highly mineralized fluorapatite ($Ca_5(PO_4)F$) enameloid layer (e.g., Enax et al. 2012). Unlike dentin, enameloid is highly resistant to diagenesis (e.g., Kolodny and Raab 1988), preserving original isotopic values even at geologic timescales (e.g., Ostrom et al. 1990, 1993; Kolodny and Luz 1991; Fischer et al. 2012, 2013; Hättig et al. 2019; Kast et al. 2022; Comans et al. 2024). Enameloid phosphate precipitates in isotopic equilibrium with body water at body temperature due to rapid, enzyme-catalyzed exchange reactions (Kolodny et al. 1983). The body water of fishes is in equilibrium with seawater (Kolodny et al. 1983), making the $\delta^{18}O_p$ of biogenic apatite phosphate in fish enamel(oid) (i.e., bony fishes and sharks) a function of the oxygen isotope composition of seawater ($\delta^{18}O_{sw}$) and body temperature at the time of tooth formation (Longinelli and Nuti 1973; Kolodny et al. 1983; Kolodny and Raab 1988). Most sharks are poikilothermic, meaning the surrounding ambient sea temperatures control their body temperatures. Thus, the $\delta^{18}O_p$ of shark enameloid should reflect ambient water-temperature conditions during tooth formation (e.g., Žigaitė and Whitehouse 2014; Karnes et al. 2024). Indeed, researchers have used the $\delta^{18}O_p$ of shark enameloid to infer environmental conditions, including seawater temperature (Kolodny and Raab 1988; Kolodny and Luz 1991; Pucéat et al. 2003; Hättig et al. 2019; Leuzinger et al. 2023) and salinity (Fischer et al. 2012, 2013; Leuzinger et al. 2015) in both modern (Vennemann et al. 2001; Kocsis et al. 2015; Tütken et al. 2020) and ancient systems (e.g., Kohn and Cerling 2002; Fischer et al. 2012; Tütken et al. 2020). Limited studies have used $\delta^{18}O_p$ to explore the paleoecology of these fossil sharks directly (e.g., Fischer et al. 2012, 2013; Griffiths et al. 2023; Larocca Conte et al. 2024).

Here we measured the $\delta^{18}O_p$ of six Late Cretaceous shark species from two formations (the offshore Mooreville Chalk and the nearshore Blufftown Formation) to investigate shark paleoecology in the Gulf Coastal Plain (GCP). The geologic formations are similar in age but with different lithologies. The sampled localities are within a relatively small geographic area and probably experienced similar environmental conditions within the GCP, which was likely in open exchange with the Atlantic Ocean. Also, many specimens of each taxon are available in museum collections from both formations for partially destructive analysis. We also compared shark tooth enameloid $\delta^{18}O_p$ values with those of tooth enamel from a co-occurring bony fish, *Enchodus petrosus* Cope, 1874, in each formation as a reference for ambient conditions (Harrell et al. 2016). We expect that sharks that spent significant time in a nearshore environment with the potential for low $\delta^{18}O$ freshwater input (e.g., brackish conditions) preserved enameloid with lower $\delta^{18}O_p$ values than those from strictly marine environments. However, sharks can be migratory, and given tooth replacement and isotopic incorporation rates (e.g., weeks to months depending on the taxon; Moss 1967; Reif et al. 1978; Bruner 1998; Zeichner et al. 2017), we consider possible sources of $\delta^{18}O_p$ variation within individuals and across taxa, including water depth and thermal gradients, migrations and latitudinal thermal gradients (e.g., Western Interior Seaway [WIS]), and variation in the $\delta^{18}O_{sw}$ (e.g., marine vs. brackish settings). In addition, although most sharks are poikilothermic, several modern taxa are recognized as having higher body temperatures than surrounding waters (e.g., great white shark, *Carcharodon carcharias*), and there is increasing evidence for thermoregulation in some Late Cretaceous sharks (Ferrón 2017; Pimiento et al. 2019), which would influence $\delta^{18}O_p$. We consider a variety of these biological and environmental influences and present here paleoecological interpretations of several Late Cretaceous sharks in the GCP.

Materials and Methods

Sampled Late Cretaceous Taxa

We sampled tooth specimens from six different shark species, including five Lamniformes (hereafter referred to as lamniforms): *Cretoxyrhina mantelli* Agassiz, 1835, *Cretalamna appendiculata* Agassiz, 1835, *Scapanorhynchus texanus* Roemer, 1849, *Squalicorax kaupi* Agassiz, 1843, *Squalicorax pristodontus* Agassiz, 1835, and *Ptychodus mortoni* Mantell, 1839. The higher taxonomic placement of the genus *Ptychodus* is debated (see Shimada 2012), and in this study, we adopt the designation *incertae sedis* (e.g., Hoffman et al. 2016). Paleontologists have proposed that the definitive Late Cretaceous lamniforms included in this study were globally distributed nektonic predators based on inferred diets, depositional environments, and similarities to modern lamniforms (e.g., Cappetta 1987; Shimada 1997a; Shimada and Cicimurri 2005; Shimada 2007). The piercing- and cutting-type lamniform teeth were likely effective for consuming a variety of prey items found in both near- and offshore environments, including marine reptiles (Schwimmer et al. 1997; Everhart 2004), bony fishes (Hamm and Shimada 2002; Ciampagalio et al. 2005), and other sharks (e.g., Shimada 1997a). *Ptychodus mortoni* is known from marine deposits in North America (United States), South America (Mexico), Europe, and Africa (e.g., Applegate 1970; Cappetta 1987; Shimada et al. 2010; Ciampagalio et al. 2013; see review of localities by Blanco-Piñón et al. 2007). Similar to modern durophagous sharks with molariform teeth, the genus *Ptychodus* is interpreted to be a benthic predator (e.g., Shimada et al. 2009, 2010) that consumed hard-shelled macroinvertebrates by crushing or crunching (Ciampagalio et al. 2005; Shimada 2012; Amadori et al. 2022), although nektonic turtles and ammonites have also been proposed as components of their diets (Vullo et al. 2024). Thus, lamniform and *P. mortoni* diets inferred from tooth morphology suggest that there may be some habitat differences or partitioning among the sampled taxa (e.g., offshore vs. nearshore, benthic vs. nektonic).

https://doi.org/10.1017/pab.2024.45 Published online by Cambridge University Press

Following the approach of Harrell et al. (2016), we used *E. petrosus* as a reference for poikilothermic fish whose $\delta^{18}O_p$ values record ambient conditions. We compared the mean shark taxon $\delta^{18}O_p$ values with those of *E. petrosus* from the same geologic formation. *Enchodus petrosus* was an active predator (Cumbaa et al. 2013) but may also have been a prey item of larger vertebrates, including sharks (e.g., Shimada 1997a; Everhart 2004), meaning it likely occupied the same habitat as the predatory sharks (e.g., Schein and Lewis 2007; McIntosh et al. 2016; Allen and Shimada 2021). Comparing shark $\delta^{18}O_p$ values with those of *E. petrosus* allows us to evaluate the direction and magnitude of any potential differences between sharks and ambient conditions and explore possible drivers of those differences.

Geologic Setting

The Mooreville Chalk and the Blufftown Formation in Alabama (Fig. 1) are temporally equivalent (latest Santonian–Campanian) but with different lithologies, and both have well-preserved marine vertebrate fossils (e.g., Applegate 1970; Case and Schwimmer 1988; Shimada and Hooks 2004; Shimada and Brereton 2007; Shimada et al. 2009; Ikejiri et al. 2013; Ehret and Harrell 2018). The Mooreville Chalk consists of yellowish-gray to dark-bluish-gray fossiliferous chalky clay and chalky marl with siliciclastic sediments near the base of the formation. The upper Arcola Limestone Member overlays the lower, undifferentiated strata of the Mooreville Chalk and consists of calcisphere wackestones and packstones (Tew 2000) and chalky marl beds (Raymond et al. 1988). Sedimentologists have interpreted the Mooreville Chalk to represent deposition in an inner to middle neritic environment (Mancini and Soens 1994; Puckett 1995; Mancini et al. 1996) with water depths ranging up to 90 m (Puckett 1991).

In Alabama, the Blufftown Formation is exposed in the eastern portion of the state (Fig. 1) and consists of gravelly, glauconitic, calcareous sand and sandy clay that grades into the Mooreville Chalk in western Alabama (Raymond et al. 1988). The Blufftown Formation was deposited in a nearshore, marginal marine environment (Skotnicki and King 1986; King 1990; Schwimmer et al. 1993; King and Skotnicki 1994), potentially with substantial freshwater input from rivers in the upper portion of the Blufftown of eastern Alabama to western Georgia (e.g., Case and Schwimmer 1988).

Sampling Approach

We sampled specimens from the Alabama Museum of Natural History (ALMNH) and the Auburn University Museum of Natural History (AUM) (see Appendix A, Supplemental Data). When possible, we sampled at least three teeth from each selected species within both formations (Table 1). Due to specimen availability, we sampled only a single *S. pristodontus* tooth and no *P. mortoni* teeth from the Blufftown Formation. We used a Dremel rotary tool with a diamond drill bit to remove the outer

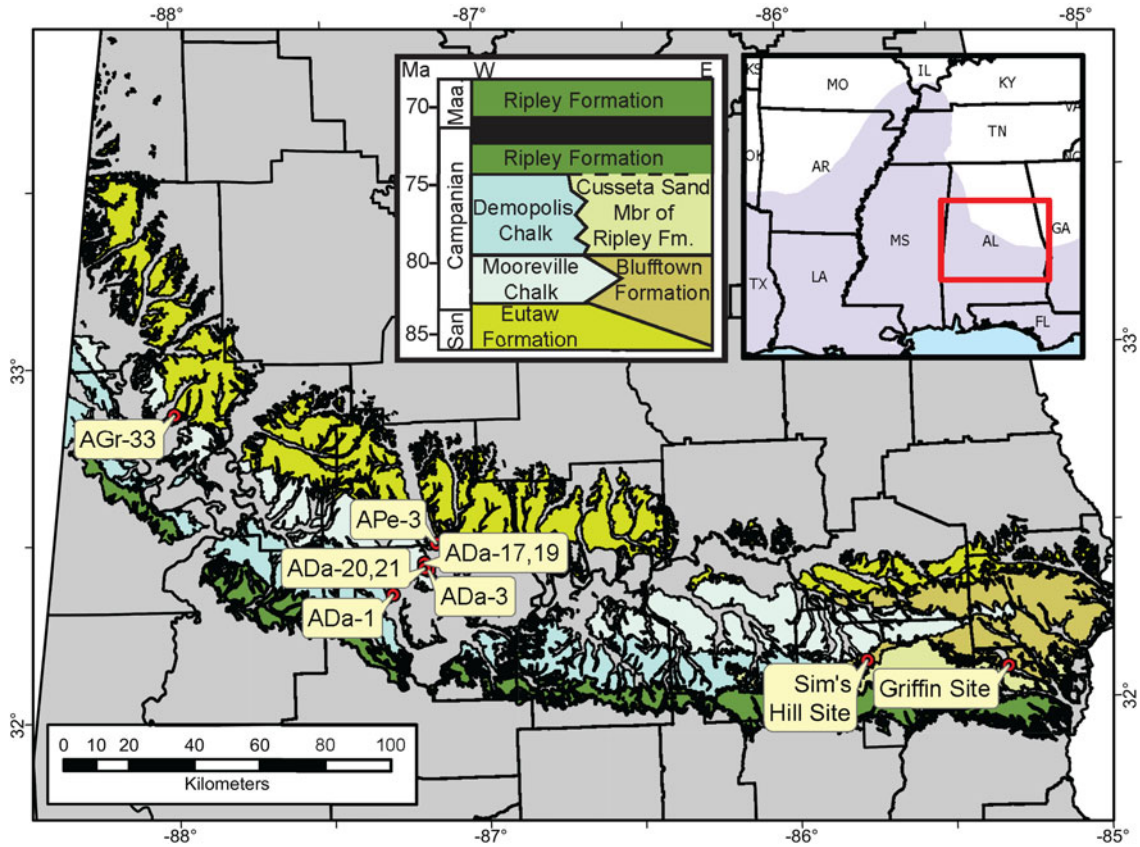

Figure 1. Map of the Late Cretaceous (Santonian–Maastrichtian) strata exposed in Alabama, USA (modified from Mohr et al. 2024) with specimen localities sampled in this study. The purple shaded area in the inset map shows the Gulf Coastal Plain. The stratigraphic column inset shows a simplified view of Late Cretaceous units from western to eastern Alabama (Raymond et al. 1988). Alabama geologic map data sourced from the Geological Survey of Alabama (Szabo et al. 1988). See Supplemental Data for locality information for each specimen.

https://doi.org/10.1017/pab.2024.45 Published online by Cambridge University Press

Table 1. Summary of the mean $\delta^{18}O_p$ values by taxon from the Mooreville Chalk and Blufftown Formation with upper and lower 95% confidence intervals (CI). Asterisks (*) indicate statistically significant offsets from co-occurring *Enchodus petrosus* averages. *N* = the number of teeth sampled per taxon. *n* = the total number of measurements per taxon. VSMOW, Vienna Standard Mean Ocean Water.

Taxon	*N*	*n*	$\delta^{18}O_p$ ‰ (VSMOW) mean	95% CI		$\delta^{18}O_p$ offset from *Enchodus*
				Lower	Upper	
Mooreville Chalk						
Enchodus petrosus	3	8	21.3	20.9	21.7	–
Cretalamna appendiculata	3	9	21.3	20.9	21.7	0.0
Cretoxyrhina mantelli	3	8	20.2	19.8	20.7	−1.1*
Squalicorax kaupi	7	17	21.7	21.5	22.0	0.4
Squalicorax pristodontus	3	8	22.0	21.6	22.4	0.7
Scapanorhynchus texanus	3	8	21.2	20.7	21.6	−0.1
Ptychodus mortoni	3	9	19.1	18.7	19.6	−2.2*
Blufftown Formation						
Enchodus petrosus	3	7	21.4	21.0	21.8	–
Cretalamna appendiculata	3	6	21.2	20.8	21.6	−0.2
Cretoxyrhina mantelli	3	8	18.1	17.7	18.5	−3.3*
Squalicorax kaupi	3	9	21.1	20.7	21.5	−0.3
Squalicorax pristodontus	1	3	21.9	21.2	22.6	0.5
Scapanorhynchus texanus	3	9	21.2	20.7	21.6	−0.2

enameloid layer, creating 300–500 µg of enameloid powder per sample. We sampled each tooth in three discrete locations: at the apex, the middle, and the base of the crown (Fig. 2). During shark tooth formation, the enameloid is first mineralized at the apex of the crown, and mineralization progresses toward the base (Jambura et al. 2019). Because enameloid thickness varies across the tooth crown, we also re-analyzed our data using only results from a single position (apical) to confirm that sampling position did not affect our results. The amount of time captured by tooth formation (i.e., isotopic incorporation rate; e.g., Kim et al. 2012; Zeichner et al. 2017) can vary across shark taxa from weeks to months (Moss 1967; Reif et al. 1978; Bruner 1998; Zeichner et al. 2017). By sampling in three different locations along the crown, we capture the isotopic history of the tooth and can assess intra-tooth variability. We also sampled teeth from *E. petrosus* using the same sampling procedure outlined earlier.

Single Individual Sampling Approach. Many modern lamniform sharks undertake migrations of hundreds to thousands of miles (e.g., Bonfil et al. 2005; Gore et al. 2008), passing through different habitats and environmental conditions. Sharks continuously shed and replace their teeth throughout their lifetimes, and a single tooth records only a narrow time interval of an individual's life. Examining multiple teeth from a single individual that are precipitated at different times, thus potentially recording various environmental conditions, can provide valuable insight into migrations or habitat changes over time. However, it is often difficult to conduct these studies due to the rarity of multiple teeth found in association from a single individual. We analyzed five

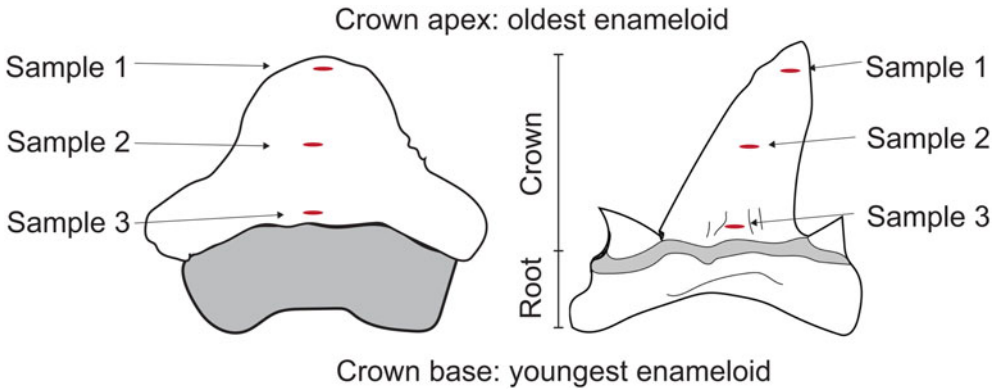

Figure 2. Individual specimen sampling strategy. Three samples were drilled from each tooth specimen from the base to the top of the enameloid crown. Sample 1 was taken from the apex, Sample 2 from the middle, and Sample 3 from the base of the crown. The tooth on the left illustrates the general shape of a *Ptychodus mortoni* crown. The tooth on the right illustrates the general shape of the lamniform *Cretalamna appendiculata*, but the sampling strategy was applied to all lamniforms sampled in this study.

https://doi.org/10.1017/pab.2024.45 Published online by Cambridge University Press

randomly chosen, disarticulated (i.e., not in situ), yet associated teeth that are interpreted to come from a single individual (*Squalicorax kaupi*; ALMNH:Paleo:2422a-e) collected from the Mooreville Chalk to assess intra-individual variability.

Stable Oxygen Isotope Analysis of Biogenic Phosphate

We processed and analyzed powdered enameloid samples at the University of Arkansas Stable Isotope Laboratory (UASIL) following the slow microprecipitation of silver phosphate (Ag_3PO_4) method adapted from O'Neil et al. (1994), Vennemann et al. (2002), and Bassett et al. (2007). We added 100 µl of 0.5 M HNO_3 to each sample and allowed samples to sit overnight to dissolve the enameloid powder. Next, we added 75 µl of 0.5 M KOH and 200 µl of 0.17 M KF to increase pH, decrease the solubility of CaF_2, and precipitate out Ca^{2+} as CaF_2. We then centrifuged samples and used disposable glass pipettes to transfer the supernatant to new, clean microcentrifuge tubes. To precipitate the Ag_3PO_4 crystals, we added 250 µl of silver ammine solution (O'Neil et al. 1994; Bassett et al. 2007) and allowed samples to sit for 21 hours in an oven at 46°C. At 21 hours, we added 1 ml of deionized water to each sample and centrifuged to prevent nitrate oxide contamination. We then decanted the supernatant. After precipitation of the silver phosphate crystals was completed, we centrifuged and rinsed samples five more times with deionized water and allowed them to dry for at least 24 hours in an oven at 46°C. After the samples were dried, we inspected each centrifuge tube of Ag_3PO_4 crystals under a microscope to assess crystal appearance and exclude samples with suspected contamination by fibers or any non-Ag_3PO_4 crystals. We analyzed Ag_3PO_4 crystals using a high-temperature conversion elemental analyzer by reacting the crystals with graphite at 1400°C to produce CO gas (Vennemann et al. 2002) that was then measured via continuous flow using a Thermo Finnigan Delta Plus XL Gas Chromatograph Isotope Ratio Mass Spectrometer (IRMS). We report our results here in standard delta notation ($\delta^{18}O$) relative to VSMOW (Vienna Standard Mean Ocean Water).

We prepared NIST SRM 120c along with enameloid samples as a quality control standard to monitor accuracy and precision (21.6 ± 1.2‰, $n = 9$). UASIL used the following reference standards: USGS-81 (34.6 ± 1.3‰, $n = 21$) and NBS-127 (8.5 ± 0.4‰, $n = 14$). The instrumental precision was 0.4‰, derived from the NBS-127 standard. We removed measurements with low mass to peak area relation (i.e., not completely Ag_3PO_4, $n = 7$ measurements) or small peaks (i.e., poorly constrained, $n = 2$ measurements) before beginning data analyses (See Appendix A, Supplemental Data).

Statistical Approach

Our data have a hierarchical structure, and we calculated our mean $\delta^{18}O_p$ values at the specimen (single-tooth) level and then used mean specimen values to calculate a taxon-level mean $\delta^{18}O_p$ value. To calculate a confidence interval, we resampled each measurement 10,000 times from a normal distribution, where the $\delta^{18}O_p$ value was the mean and the instrumental precision (0.4‰) was the standard deviation. For each resampling iteration, we calculated mean $\delta^{18}O_p$ values for each specimen and subsequently, from each specimen mean, each taxon mean within each formation. Standard deviations for specimen and taxon mean $\delta^{18}O_p$ values were calculated from the standard deviation of calculated values from all resampling iterations. Almost all calculated specimen and taxon $\delta^{18}O_p$ values had standard deviations below instrumental precision (0.4‰). To be conservative, we increased (to 0.4‰) the standard deviation for any calculated specimen or taxon standard deviation values that were below this instrumental precision. Higher values were not modified. Next, we followed the same resampling approach to estimate the offsets between shark taxa and *E. petrosus* $\delta^{18}O_p$ mean values (i.e., shark mean minus *E. petrosus* mean). We resampled offset means and standard deviations using the previously calculated mean taxon values and standard deviations. Finally, we tested the significance of offsets between shark taxa and *E. petrosus* using analysis of variance and post hoc Tukey's honestly significant difference (HSD) tests. We observed identical offsets between sharks and *E. petrosus* when we resampled our data following the same procedure but using two random values from each specimen, confirming the adequacy of our physical sampling scheme (Fig. 2). We used an α value of 0.05 for all tests and completed all statistical analyses using RStudio v. 4.2.1 (R Core Team 2022).

Results

Shark $\delta^{18}O_p$ Offsets from Enchodus petrosus

Mooreville Chalk. Summary $\delta^{18}O_p$ values for each taxon in the Mooreville Chalk are shown in Table 1. *Cretalamna appendiculata*, *Scapanorhynchus texanus*, *Squalicorax kaupi*, and *Squalicorax pristodontus* have $\delta^{18}O_p$ values that are statistically indistinguishable from co-occurring *E. petrosus* (21.3‰; see Table 1). Post hoc Tukey HSD tests for multiple comparisons found $\delta^{18}O_p$ values are significantly different between only *Ptychodus mortoni–E. petrosus* and *Cretoxyrhina mantelli–E. petrosus* ($p < 0.01$ and $p = 0.04$, respectively; Fig. 3, Table 1, Supplementary Table 1). *Ptychodus mortoni* $\delta^{18}O_p$ is 1.1‰ lower and *C. mantelli* $\delta^{18}O_p$ is 2.2‰ lower than co-occurring *E. petrosus* $\delta^{18}O_p$ (Fig. 3, Table 1). The $\delta^{18}O_p$ values for *C. mantelli* and *P. mortoni* are nearly, but not significantly different from each other (Student's *t*-test: $t = 2.51$, df = 4, $p = 0.06$). There are no differences in $\delta^{18}O_p$ values between shark specimens from the Arcola Limestone Member of the Mooreville Chalk and the reference *E. petrosus* from the lower unnamed Mooreville Chalk (Student's *t*-test: $t = -1.3$, df = 16, $p = 0.2$).

Blufftown Formation. Summary $\delta^{18}O_p$ values for each taxon in the Blufftown Formation are shown in Table 1. Similar to the Mooreville Chalk, *C. appendiculata*, *S. texanus*, *S. kaupi*, and *S. pristodontus* have overlapping $\delta^{18}O_p$ values with co-occurring *E. petrosus* (21.4‰; see Table 1). Post hoc Tukey HSD tests for multiple comparisons found $\delta^{18}O_p$ values are significantly different only between *C. mantelli–E. petrosus* (−3.3‰ difference, $p \ll 0.01$; Fig. 3, Table 1). *Cretoxyrhina mantelli* is also the only taxon sampled from both formations to have significantly different $\delta^{18}O_p$ values between the formations (Student's *t*-test: $t = 3.17$, df = 4, $p = 0.03$; Fig. 4;).

$\delta^{18}O_p$ Variability

Intra-individual Variability. The five teeth measured from a single *S. kaupi* individual from the Mooreville Chalk have a mean $\delta^{18}O_p$ value of 22.2‰ and a range of 2.1‰ (20.8‰ to 22.9‰; Supplementary Fig. 1), much higher than previously reported intra-individual variations (up to 1.1‰; Vennemann et al. 2001), and higher than any intra-taxon variability observed within

https://doi.org/10.1017/pab.2024.45 Published online by Cambridge University Press

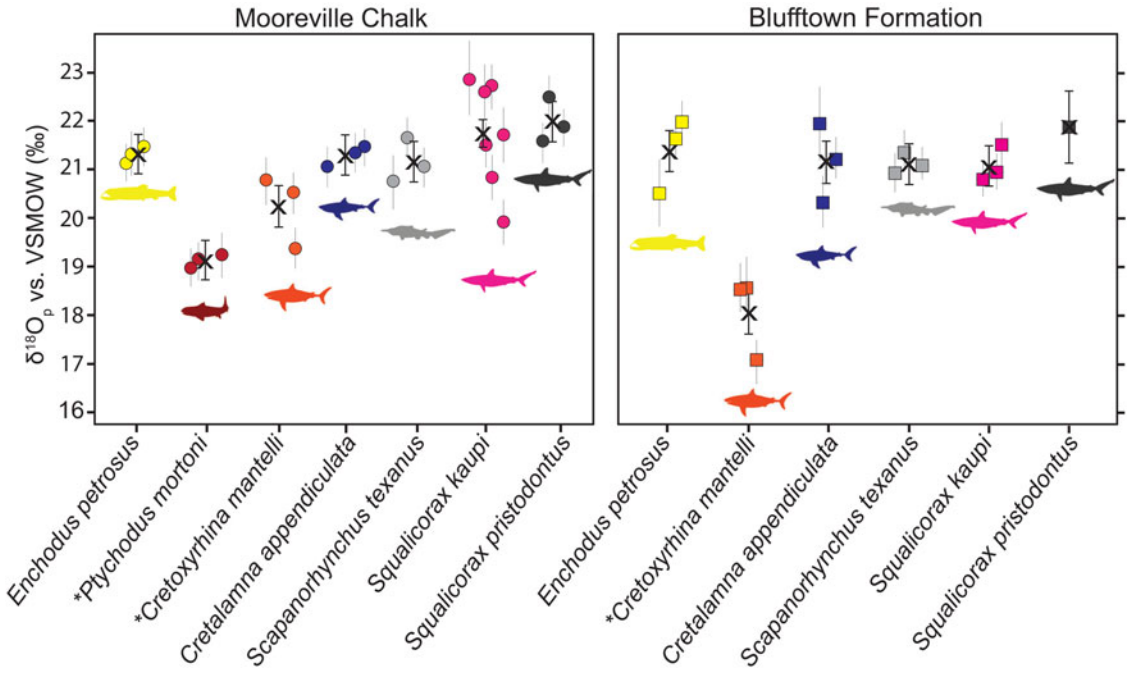

Figure 3. Mean specimen (circle) and taxon (X) $\delta^{18}O_p$ values from the Mooreville Chalk and the Blufftown Formation. Bracketed vertical lines indicate 95% confidence intervals (CIs) of the taxon mean. Light gray vertical bars indicate 95% CIs of the specimen mean. Asterisks (*) on taxon names indicate that the mean isotopic composition of those taxa are significantly different from the mean of the co-occurring fish *Enchodus petrosus*. VSMOW, Vienna Standard Mean Ocean Water. The image silhouettes are from PhyloPic (https://www.phylopic.org) and were contributed as follows: *Cretoxyrhina mantelli* by Dmitry Bogdanov (2013; CC BY 3.0), and the orignal color was changed from black to orange; *Cretalamna appendiculata* by Oliver E. Demuth and Cooper et al. (2020) (2023; CC BY 4.0), and the original color was changed from black to blue; and *Scapanorhynchus texanus* by Dianne Bray/Museum of Victoria (2013; CC BY 3.0), and the original color was changed from black to grey.

a formation (Supplementary Table 2). Specimens ALMNH:Paleo:2422d and ALMNH:Paleo:2422e have significantly different mean values from the other three teeth sampled but have $\delta^{18}O_p$ values consistent with co-occurring *E. petrosus* (Supplementary Fig. 1). Specimens ALMNH:Paleo:2422b and ALMNH:Paleo:2422d have the highest intra-tooth variability, but variability within all five teeth from the single *S. kaupi* individual is less than 0.5‰.

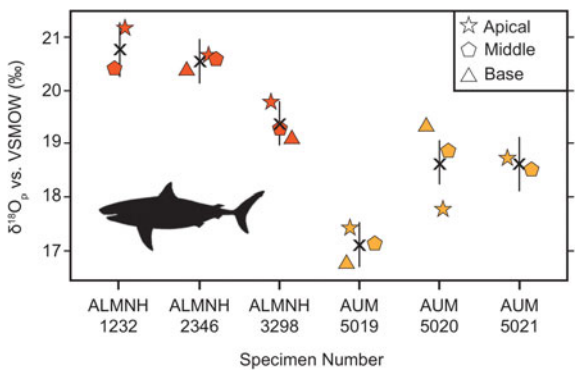

Figure 4. Individual measurements per specimen and mean tooth (X) $\delta^{18}O_p$ values for *Cretoxyrhina mantelli* specimens from the Mooreville Chalk (dark orange) and the Blufftown Formation (light orange). Black vertical lines indicate 95% confidence intervals of each specimen mean. Tooth crown sample positions: apical (stars), middle (pentagons), and base (triangles). ALMNH, Alabama Museum of Natural History; AUM, Auburn University Museum of Natural History; VSMOW, Vienna Standard Mean Ocean Water. The image silhouette is from PhyloPic (https://www.phylopic.org) and was contributed by Dmitry Bogdanov (2013; CC BY 3.0).

Discussion

Most shark taxa sampled here were likely poikilothermic and living in open-marine environments, as evidenced by the overlapping $\delta^{18}O_p$ values of taxa within and between the Mooreville Chalk and the Blufftown Formation (Fig. 3, Table 1, Supplementary Table 1). Within both formations, *Cretalamna appendiculata*, *Scapanorhynchus texanus*, *Squalicorax kaupi*, and *Squalicorax pristodontus* have $\delta^{18}O_p$ values indistinguishable from the bony fish, *Enchodus petrosus*. While many sharks can migrate vast distances, potentially recording a variety of environmental conditions, the low intra-taxon variability of those taxa measured here (Supplementary Table 2) would indicate that most taxa spent substantial time in the GCP, at least relative to their tooth replacement rates. An exception to this generality is the poikilothermic *S. kaupi* individual that has teeth with significantly different $\delta^{18}O_p$ values (Supplementary Fig. 1) and large intra-individual variability (2.1‰) that suggests migration between different environments (e.g., higher and lower latitudes within the Northern Atlantic Ocean; Cappetta 1987, 2012). The difference in isotopic histories between a single tooth and multiple teeth from a single individual can provide greater insight into migration or habitat shifts over time, but articulated shark jaws are rare and generally not available for destructive sampling for isotope analyses.

We observe significant differences in *Ptychodus mortoni* and *Cretoxyrhina mantelli* $\delta^{18}O_p$ values from co-occurring *E. petrosus* $\delta^{18}O_p$ values in the Mooreville Chalk and the Blufftown Formation. These offsets from *E. petrosus* are likely not the result of differences in environmental conditions between the formations, because the $\delta^{18}O_p$ values for *E. petrosus* are similar in

https://doi.org/10.1017/pab.2024.45 Published online by Cambridge University Press

each unit. Rather, these offsets likely result from variations in $\delta^{18}O_{sw}$ or temperature due to differences in the habitats or biology of these taxa specifically. Species-specific nonequilibrium isotope biologic fractionation effects (i.e., kinetic effects), sometimes called "vital effects," could explain these differences, but we are unable to recognize such vital effects over and above those of biological or habitat signals. Vennemann et al. (2001) investigated possible $\delta^{18}O_p$ vital effects in several modern shark species (including lamniforms) and found little evidence of vital effects distinguishable from habitat or biological signals. Žigaitė and Whitehouse (2014) demonstrated the effects of tooth histology and ontogeny on the $\delta^{18}O_p$ of modern sandbar shark (*Carcharhinus plumbeus*) enameloid and dentin precipitated under controlled conditions and concluded that enameloid was a reliable recorder of ambient environmental conditions. Because disequilibrium vital effects have not been documented, and paleotemperature reconstructions from $\delta^{18}O_p$ of shark enameloid are generally consistent with other proxies (e.g., Kolodny and Raab 1988; Roelofs et al. 2017; Hättig et al. 2019), we consider this explanation unlikely to explain the observed offsets.

In the following sections, we address ecological explanations for the divergent $\delta^{18}O_p$ values, with a particular focus on the anomalous taxa *P. mortoni* and *C. mantelli*. First, we consider explanations driven by different $\delta^{18}O_{sw}$ values these taxa could encounter in other habitats; second, we consider explanations driven by different temperatures these taxa could either encounter or generate internally.

$\delta^{18}O$ of Seawater

If the negative *P. mortoni–E. petrosus* and *C. mantelli–E. petrosus* offsets are driven solely by differences in $\delta^{18}O_{sw}$ values, we can calculate the required $\delta^{18}O_{sw}$ values using the relationship between temperature, $\delta^{18}O_{sw}$, and $\delta^{18}O_p$ and holding temperature constant (e.g., Lécuyer et al. 2013):

$$T_{body}(^{\circ}C) = 117.4 - 4.5*(\delta^{18}O_p - \delta^{18}O_{sw}) \quad (1)$$

For a constant temperature, differences in $\delta^{18}O_p$ equate exactly to the same magnitude difference in $\delta^{18}O_{sw}$. If we assume a $\delta^{18}O_{sw}$ of −1‰ for an ice-free Late Cretaceous (e.g., Shackleton and Kennett 1975), the *P. mortoni–E. petrosus* offset in the Mooreville Chalk indicates a $\delta^{18}O_{sw}$ of −3.2‰, and the *C. mantelli–E. petrosus* offsets in the Mooreville Chalk and the Blufftown Formation indicate $\delta^{18}O_{sw}$ of −2.1‰ and −4.2‰, respectively. These lower $\delta^{18}O_{sw}$ values could be explained by increased local freshwater influence or migration from areas with lower open-marine $\delta^{18}O_{sw}$ values, which we explore below.

Freshwater Influence. The low *P. mortoni* and *C. mantelli* $\delta^{18}O_p$ values could be explained by some time spent in a brackish environment. A previous study used the $\delta^{18}O_p$ of hybodont shark enameloid from the Late Triassic Rhaetian Sea to show the transition from marine to nonmarine conditions within the region, supporting euryhalinity (i.e., tolerance for a wider range of salinities) in certain hybodont taxa (Fischer et al. 2012). Although our data imply that the Blufftown Formation is open marine with normal salinity, areas of nearby brackish conditions in the GCP are implied by frequent (e.g., biweekly) negative $\delta^{18}O_p$ excursions from in situ mosasaur teeth, which were interpreted to represent short migrations into local areas of fresher water (Taylor et al. 2021). We cannot sample a similar articulated jaw for sharks, but the consistently lower $\delta^{18}O_p$ values from *P. mortoni* and *C. mantelli* individuals could be explained if they inhabited or spent substantial time in brackish conditions.

Most modern marine sharks, except for the bull shark (*Carcharhinus leucas*, Carcharhiniformes) are stenohaline (i.e., tolerant of a narrow range of salinities). After time spent in 75% seawater (i.e., 25% freshwater), stenohaline sharks (e.g., *Heterodontus portusjacksoni*, *Mustelus antarcticus*) suffer a significant decrease in urea and blood oxygen that can compromise osmoregulation (Cooper and Morris 2004; Morash et al. 2016). If we apply this 25% freshwater (75% seawater) threshold to stenohaline Late Cretaceous sharks and assume a $\delta^{18}O_{sw}$ of −1‰ with a $\delta^{18}O$ of freshwater of −9‰ in the eastern GCP (e.g., Poulsen et al. 2007), then we may expect that stenohaline sharks in the GCP could tolerate an average local $\delta^{18}O_{sw}$ as low as −3‰ (or an offset of −2‰ from our *E. petrosus*). Offsets from *E. petrosus* beyond −2‰ (i.e., more negative) could indicate tolerance of a wider range of salinities. Thus, while the smaller *C. mantelli–E. petrosus* offset in the Mooreville Chalk (−1.1‰) could be explained by some time in a brackish environment within standard shark salinity tolerance limits, the larger offset in the Blufftown Formation (−3.3‰) would require a living environment that was fresher than most sharks can tolerate (Table 1). The *P. mortoni–E. petrosus* offset in the Mooreville Chalk (−2.2‰) is plausibly consistent (within uncertainty) with a brackish-water habitat for *P. mortoni*, albeit at the lower edge of salinity tolerances for most sharks (see "$\delta^{18}O$ of Seawater").

While the isotopic results of this study are consistent with *P. mortoni* inhabiting brackish conditions over long periods, we consider this explanation unlikely for several reasons. First, *P. mortoni* is known only from marine deposits (see "Sampled Late Cretaceous Taxa"). Further, *P. mortoni* from the Eutaw Formation (Alabama, USA; Fig. 1) had lower nitrogen isotope values from enameloid-bound organic matter ($\delta^{15}N_{EB}$) than co-occurring marine lamniforms (Comans et al. 2024), inconsistent with the higher $\delta^{15}N_{EB}$ values expected in estuarine conditions (Shipley et al. 2021). Second, we might expect sharks like *C. leucas* that transition between marine and brackish settings (e.g., Heupel and Simpfendorfer 2008; Smoothey et al. 2019) to have a greater range of $\delta^{18}O_p$ values, because their teeth would incorporate different environmental conditions during their lifetimes (e.g., Žigaitė and Whitehouse 2014). *Ptychodus mortoni* specimens have a very small $\delta^{18}O_p$ range (0.3‰; Supplementary Table 2), implying they remained in one location rather than transitioning between different environments. Given the lack of physical evidence for their presence in brackish environments, their measured $\delta^{15}N_{EB}$ values, low interspecimen $\delta^{18}O_p$ variability, and the rarity of euryhaline tolerance in sharks, we do not consider occasional migrations or full-time occupancy of a brackish habitat as a likely explanation for the *P. mortoni–E. petrosus* offset in the Mooreville Chalk.

Similarly, the lower $\delta^{18}O_p$ values recorded for *C. mantelli* from both formations could potentially be explained by differences in time spent in brackish conditions, although we also consider this explanation implausible for this taxon. Ontogenetic habitat partitioning, wherein juveniles inhabited nearshore environments while adults lived offshore, could explain the lower $\delta^{18}O_p$ values in the Blufftown Formation if those specimens are juveniles. Researchers have observed such habitat partitioning in the modern *Carcharodon carcharias* and *Isurus oxyrinchus* (Hoyos-Padilla et al. 2016; Tamburin et al. 2019), which are modern analogues

https://doi.org/10.1017/pab.2024.45 Published online by Cambridge University Press

for *C. mantelli* (Shimada 1997a,b). However, adult individuals from either of these modern species are not known to inhabit brackish or freshwater, and we interpret the *C. mantelli* teeth sampled from each formation in this study to represent adult individuals. Further, *C. mantelli* specimens are known only from marine strata (see "Sampled Late Cretaceous Taxa"). The larger (−3.3‰) $\delta^{18}O_p$ offset for this taxon in the Blufftown Formation would require ~40% freshwater contribution, which would be difficult for most sharks to tolerate. Additionally, the inferred prey items of *C. mantelli* based on predator–prey interactions in the fossil record (e.g., Shimada 1997a; Shimada and Hooks 2004) indicate a primarily marine habitat. Thus, inferences from modern analogues, the lack of *C. mantelli* specimens collected from nonmarine or estuarine environments, and an inferred diet of marine prey do not support the freshwater hypothesis or account for differences in $\delta^{18}O_p$ values between formations.

$\delta^{18}O_{sw}$ Variation and Migration. A nearby brackish habitat is an unlikely explanation for the anomalously low *P. mortoni* and *C. mantelli* $\delta^{18}O_p$ values, but there could have been a $\delta^{18}O_{sw}$ gradient between surface and bottom waters (e.g., Craig 1966; Woo et al. 1992) in the GCP due to evaporative effects. However, a surface to bottom water difference would result in higher $\delta^{18}O_p$ values, not lower, for surface-dwelling nektonic sharks. Alternatively, either *P. mortoni* or *C. mantelli* could have spent substantial time in fully marine environments with lower $\delta^{18}O_{sw}$ values relative to the GCP (e.g., the more normal marine WIS). In this model, the organism would have grown teeth in the WIS before migrating to the GCP and losing teeth there, which could explain both shark taxon–*E. petrosus* offsets as well as the *C. mantelli* $\delta^{18}O_p$ differences between formations. Both *C. mantelli* (e.g., Shimada 1997a) and *P. mortoni* (Shimada et al. 2010) have biogeographic distributions that include the WIS (see "Sampled Late Cretaceous Taxa"). If we consider the proximity of the WIS to the GCP and that each tooth represents weeks to months of an individual's life, then it is feasible that individuals migrated from lower $\delta^{18}O_{sw}$ waters of the WIS to higher $\delta^{18}O_{sw}$ waters of the GCP. Indeed, previously reported WIS $\delta^{18}O_{sw}$ values (−8‰ to −1‰) are consistent with the $\delta^{18}O_{sw}$ values estimated for our measured specimens (e.g., Coulson et al. 2011; Peterson et al. 2016; see "$\delta^{18}O$ of Seawater"). Thus, given our understanding of shark biology, migration from marine waters with lower $\delta^{18}O_{sw}$ (likely the WIS) is a more likely explanation than more local $\delta^{18}O_{sw}$ variation driven by a local brackish habitat for the lower *P. mortoni* and *C. mantelli* $\delta^{18}O_p$ values. However, given tooth replacement rates, if migration from the WIS explains the lower $\delta^{18}O_p$ values, we also expect to find that some teeth from these organisms represent local GCP conditions in their $\delta^{18}O_p$ (i.e., $\delta^{18}O_p$ values similar to *E. petrosus*), but we do not (Fig. 3). Additionally, this model would require that lower WIS $\delta^{18}O_{sw}$ values were not associated with significantly brackish conditions, and this seems likely, given the abundance of marine taxa recovered from the WIS. Freshwater input to the WIS likely had drastically lower $\delta^{18}O$ values (e.g., Fricke et al. 2010), so even relatively small freshwater volumes could strongly influence $\delta^{18}O_{sw}$.

Temperature

Differences in tooth formation temperatures, rather than changes in $\delta^{18}O_{sw}$, could explain the shark–*E. petrosus* offsets. We can estimate the required temperature difference to generate the magnitude and direction of $\delta^{18}O_p$ offsets at the time of tooth formation by holding the $\delta^{18}O_{sw}$ constant using equation (1). The offsets for *C. mantelli* (−1.1‰) and *P. mortoni* (−2.2‰) from *E. petrosus* in the Mooreville Chalk equate to approximately a 5.0°C and 9.9°C temperature increase, respectively, above ambient conditions in the GCP. The *C. mantelli–E. petrosus* offset in the Blufftown Formation (−3.3‰) equates to a 14.9°C temperature increase above local water habitat (Table 1). Temperature differences could be achieved by occupying different water depths, migration from different locations or water currents, or warmer body temperatures relative to surrounding water temperatures.

Water Depth and Thermal Gradients. Modern and fossil shark taxa occupy a range of depths in the water column, including benthic habitats where sea temperatures may be lower than surface waters, but these differences in depth are probably not sufficient to explain the $\delta^{18}O_p$ offsets between *P. mortoni–E. petrosus* and *C. mantelli–E. petrosus*. The GCP region was likely too shallow during the Late Cretaceous to have a substantial thermal gradient (see "Geologic Setting"). Furthermore, modern temperature–depth gradients in the Gulf of Mexico indicate no substantial thermal gradient in the upper 100 m (Forrest et al. 2005; Christie and Nagihara 2016). Moreover, in most marine habitats, benthic environments are colder than the overlying surface waters, which would result in higher $\delta^{18}O_p$ values of organisms living at or near the seafloor. We observe significantly lower $\delta^{18}O_p$ values for *P. mortoni* and *C. mantelli* compared with *E. petrosus* values, indicating warmer, not cooler temperatures (Fig. 3). In addition, we do not observe a significant difference between *S. texanus* and *E. petrosus* in either formation, as expected based on morphological similarities between *S. texanus* and the modern analogue goblin shark (*Mitsukurina owstoni*) (Welton and Farish 1993), a deep-water, benthopelagic shark still found in the Gulf of Mexico today (e.g., Parsons et al. 2002). Thus, differences in $\delta^{18}O_p$ values due to habitat partitioning within the water column are not good explanations for the magnitude or the direction of the *P. mortoni–E. petrosus* and *C. mantelli–E. petrosus* offsets.

Migration from Warmer Water. Migration from warmer tropical waters could also explain the lower *P. mortoni* and *C. mantelli* $\delta^{18}O_p$ values, as both taxa are known from lower-latitude subtropical regions (see "Sampled Late Cretaceous Taxa"). A $\delta^{18}O_{sw}$ of −1‰ is commonly used for the global ocean in an "ice-free" world like that of the Cretaceous (Shackleton and Kennett 1975), but this value implies water temperatures of 16.6°C to 17.1°C for *E. petrosus* tooth formation (using equation 1), which is lower than expected for the GCP (Liu 2009; Harrell et al. 2016). Harrell et al. (2016) argued that the GCP had a higher $\delta^{18}O_{sw}$ (0‰) due to evaporative enrichment, from which they calculated a *Enchodus* sp. tooth formation temperature of 28.3°C, using the equation of Pucéat et al. (2010). Using equation (1) and a $\delta^{18}O_{sw}$ of 0‰, we calculated water temperatures of 21.1°C to 21.6°C, which is more consistent with other temperature estimates for the GCP (Coulson et al. 2011; Peterson et al. 2016). Pucéat et al. (2007) calculated sea-surface temperatures of up to 30°C for latitudes of 10–15°N using the $\delta^{18}O_p$ from bony fish ($\delta^{18}O_{sw}$ of −1‰ and the equation of Kolodny et al. [1983]). Thus, there is likely to be an approximately 9°C temperature difference (equivalent to a −2‰ $\delta^{18}O_p$ offset from *E. petrosus*) from the subtropical GCP to the tropical region. Based on this approximate latitudinal range of temperatures and estimated temperature offsets from shark $\delta^{18}O_p$ (see "Temperature"), migration from warmer lower-latitude waters could explain the *C. mantelli–E.*

https://doi.org/10.1017/pab.2024.45 Published online by Cambridge University Press

petrosus (−1.1‰) and *P. mortoni–E. petrosus* (−2.2‰) offsets in the Mooreville Chalk but is likely insufficient to fully explain the *C. mantelli–E. petrosus* (−3.3‰) offset in the Blufftown Formation (Table 1).

Although migration from warmer tropical settings could explain the observed $\delta^{18}O_p$ offsets, individuals may not have needed to migrate farther than the Western Atlantic to find waters warmer than those of the GCP. The presence of a warm-water paleo–Gulf Stream in the late Campanian to Maastrichtian has been previously proposed (Watkins and Self-Trail 2005) and may have been enhanced due to major ocean circulation changes associated with the formation of deep water in low and high latitudes (Linnert and Mutterlose 2009). Exploitation of warm-water ocean currents such as the Gulf Stream have been observed in the modern shark *C. carcharias* (e.g., Gaube et al. 2018), where warm, nutrient-rich currents not only provide access to prey but also reduce the metabolic demands of thermoregulation. The Late Cretaceous *C. mantelli* may have exploited the paleo–Gulf Stream in a similar way, but this model seems less likely for durophagous *P. mantelli* that would likely have remained in shallow-marine settings where there was an abundance of hard-shelled macroinvertebrate prey. Additionally, we would expect to find that at least some of the teeth from these organisms record isotopic values consistent with local conditions.

Body Temperature. Higher temperatures during tooth formation may also be driven by increased internal body temperatures (endothermy) of the sharks above ambient conditions. Most sharks are poikilothermic, but all modern species in the Lamnidae family (e.g., *C. carcharias* and *I. oxyrinchus*) and common thresher shark (*Alopias vulpinus*, Alopiidae: Lamniformes) maintain core body temperatures 3°C to 25°C above ambient temperatures (Carey et al. 1982; Goldman 1997; Bernal et al. 2001; Carlson et al. 2004; Bernal and Sepulveda 2005) using a vascular countercurrent heat exchange with aerobic swimming muscles in the shark's core (i.e., regional endothermy, or mesothermy as defined by Ferrón [2017]). There is paleontological evidence (e.g., phylogenies, estimated swimming speeds, and energetic budgets) that suggests Late Cretaceous otodontids (e.g., *Cretalamna*) and cretoxyrhinids (e.g., *Cretoxyrhina*) were mesothermic (e.g., Ferrón 2017; Pimiento et al. 2019). Notably, we do not observe statistically significant offsets between *C. appendiculata–E. petrosus* in either formation (Table 1), as expected based on previous studies. However, the magnitude of temperature difference in the shark's mouth over ambient temperatures, and therefore recorded by enameloid, is unclear, as body heat diffuses from the core muscles in the anterior and posterior directions (Carey and Teal 1969; Carey et al. 1982). Recent *Otodus megalodon* enameloid $\delta^{18}O_p$ values yielded body temperatures 7–8°C warmer than ambient conditions (Griffiths et al. 2023), providing quantitative evidence for the possible magnitude of mesothermy in fossil otodontid taxa. Here, an 8°C increase from mesothermy would result in an approximately −1.8‰ offset from co-occurring *E. petrosus*. Thus, mesothermy is consistent in magnitude and direction with the observed *P. mortoni* and *C. mantelli* offsets in the Mooreville Chalk but may be insufficient to fully explain the magnitude of the *C. mantelli* offset in the Blufftown Formation.

Ptychodus mortoni was a gigantic shark (Shimada et al. 2010; Shimada 2012; i.e., total body lengths greater than 6 m as defined by Pimiento et al. [2019] and Shimada et al. [2021]), which may be sufficient to explain increased body temperature through mesothermy. Pimiento et al. (2019) proposed mesothermy and filter feeding (i.e., dietary exploitation) as the two primary pathways to gigantism in sharks and suggested a single origin of shark mesothermy in Cretaceous lamniforms. Due to unresolved phylogenies, those authors did not include *C. mantelli* or *P. mortoni* in their analyses but noted that future inclusion of those species could alter conclusions on the evolution of mesothermy in sharks. Indeed, our *P. mortoni* $\delta^{18}O_p$ values in the Mooreville Chalk (19.1 ± 0.4‰; Table 1) overlap with previously reported $\delta^{18}O_p$ values for the endothermic mosasaur *Platecarpus* in the Mooreville Chalk (19.5 ± 0.2‰; Harrell et al. 2016). *Ptychodus mortoni* could have passively retained heat via gigantothermy (i.e., low surface area-to-body volume ratio that allows for passive heat retention; e.g., Paladino et al. 1990; Harrell et al. 2016; Ferrón 2017) as an alternative to active heating (i.e., mesothermy). If *P. mortoni* was gigantic because its specialized durophagy allowed it to efficiently exploit its environment, similar to extant filter feeders, then gigantothermy may be the result of its large size. While our dataset is insufficient to address the question of active versus passive heating, some form of thermoregulation is a biologically plausible explanation for lower *P. mortoni* $\delta^{18}O_p$ values.

Mesothermy can also explain the *C. mantelli–E. petrosus* offset in the Mooreville Chalk, but mesothermy alone is probably insufficient to explain the *C. mantelli–E. petrosus* offset in the Blufftown Formation (−1.1‰ and −3.3‰, respectively; Table 1, Supplementary Table 1). Cretaceous cretoxyrhinids and otodontids are likely to be phylogenetically close to modern mesothermic lamnid sharks (e.g., Cappetta 1987, 2012; Siverson et al. 2015; Ferrón 2017) and have been suggested to be mesothermic (Ferrón 2017). Given associated uncertainty, the *C. mantelli* temperature increase of 5.0°C in the Mooreville Chalk overlaps with the estimated up to 8°C body temperature increase in mesothermic sharks. Indeed, the fusiform body shape and gigantic body size (e.g., Shimada 1997b), increased swimming speed (e.g., Shimada 1997b; Amalfitano et al. 2019), large latitudinal range (e.g., Case and Baird 1990; Siverson 1992), and inferred high trophic level (Shimada 1997a) all support a possible mesothermic interpretation of our *C. mantelli* $\delta^{18}O_p$ data. However, the 14.9° C temperature increase estimated for *C. mantelli* in the Blufftown Formation is nearly 7°C warmer than expected for mesothermy alone. Mesothermy in addition to other influence(s) is a more likely explanation than mesothermy alone to explain both *C. mantelli* offsets.

Preferred Hypotheses

Ptychodus mortoni. We consider the higher body temperature hypothesis to be the most likely explanation for the anomalous *P. mortoni* $\delta^{18}O_p$ values in the Mooreville Chalk, although we cannot ascertain whether a higher body temperature was a cause or a consequence of their gigantic size. If *P. mortoni* was indeed mesothermic, it would mark a second possible occurrence of mesothermy evolving in Late Cretaceous sharks. Future studies could compare $\delta^{18}O_p$ or estimated body temperatures as a function of total body length for different *P. mortoni* specimens to investigate mesothermy versus gigantothermy. Other explanations explored earlier are consistent with our isotopic results, but we consider them less consistent with other paleontological and isotopic evidence.

Cretoxyrhina mantelli. We propose that the most likely explanation for the *C. mantelli–E. petrosus* offsets are the result of a

https://doi.org/10.1017/pab.2024.45 Published online by Cambridge University Press

combination of migration and mesothermy, because the very low $\delta^{18}O_p$ values for this taxon in the Blufftown Formation are too low for either explanation alone to be plausible. The potential phylogenetic relationship between *C. mantelli*, the mesothermic *O. megalodon*, and modern mesothermic Lamnidae sharks (e.g., Cappetta 1987, 2012; Siverson et al. 2015; Ferrón 2017) along with body morphology (e.g., Shimada 1997a,b) and function (Ferrón 2017), and a global biogeographic range all support *C. mantelli* being potentially migratory and mesothermic. One likely but equivocal explanation is that the approximately 1‰ offset in both formations is driven by endothermy, and the larger offset in the Blufftown Formation also reflects exploitation by *C. mantelli* of nearby warmer water masses, such a paleo–Gulf Stream. Future studies should compare *C. mantelli* $\delta^{18}O_p$ values with co-occurring endothermic and poikilothermic taxa, particularly in cooler, high-latitude localities, to confirm mesothermy and estimate the degree of warming.

Conclusions

Most of the fossil shark $\delta^{18}O_p$ values in this study are consistent with *Enchodus petrosus* $\delta^{18}O_p$ values, indicating similar or overlapping habitats of sharks and the predatory bony fish that we assume was poikilothermic. However, measurements of multiple teeth from a single *Squalicorax kaupi* individual indicate possible migration from cooler, higher-latitude waters or waters with a higher $\delta^{18}O_{sw}$. We also observe statistically significant negative differences between *Ptychodus mortoni* and *E. petrosus* in the Mooreville Chalk and *Cretoxyrhina mantelli* and *E. petrosus* in both the Mooreville Chalk and the Blufftown Formation. The significantly different *P. mortoni* $\delta^{18}O_p$ values are best explained by increased body temperature, either active (mesothermy) or passive (gigantothermy). Low *C. mantelli* $\delta^{18}O_p$ values are best explained by a combination of migration (either from warm, low-latitude waters, the warm currents of the paleo–Gulf Stream, or low-$\delta^{18}O_{sw}$ waters in the WIS) and mesothermy. If *P. mortoni* was mesothermic, then it would mark a second evolution of mesothermy in Late Cretaceous sharks that is potentially outside the lamniform sharks. In future studies, similar approaches including comparisons with poikilothermic fishes should be applied to studying the potential degree of mesothermy in *C. mantelli*, particularly in higher-latitude, lower-temperature paleogeographic settings, where a clearer mesothermic signal might be observed.

Acknowledgments. We thank A. Klompmaker and the Alabama Museum of Natural History, as well as R. Wilhite and D. Laurencio and the Auburn University Museum of Natural History, for allowing study and sampling of specimens from their collections. We thank the Alabama Stable Isotope Laboratory for allowing use of their equipment for sampling. We thank C. Suarez and E. D. Pollock at the University of Arkansas Stable Isotope Laboratory for their help with sample analysis. This study was funded by the Geological Society of America, the Palaeontological Society, the University of Alabama Graduate School, and the Department of Geological Sciences at the University of Alabama. We thank two anonymous reviewers for their feedback, which significantly improved the article.

Competing Interests. The authors declare that they have no competing interests.

Data Availability Statement. All data and supplementary information are available on Dryad at https://doi.org/10.5061/dryad.nvx0k6f00 and on Zenodo at https://doi.org/10.5281/zenodo.11068191.

Literature Cited

Agassiz, J. L. R. 1835. Rapport sur les poissons fossiles découverts depuis la publication de la troisième livraison. Pp. 39–64 *in Feuilleton additionel sur les Recherches sur les poissons fossiles, Quatrième* livraison. Imprimerie de Patitpierre, Neuchatel.

Agassiz, J. L. R. 1843. *Reserches sur les poissons fossils*. Imprimerie de Patitpierre, Neuchatel. P. 1420.

Allen, J. G., and K. Shimada. 2021, Fossil vertebrates from a unique marine bonebed of the Upper Cretaceous Smoky Hill Chalk, western Kansas, U.S.A.: new insights into the paleoecology of the Niobrara Formation. *Journal of Vertebrate Paleontology* **41**:e2066999.

Amadori, M., R. Kindlimann, E. Fornaciari, L. Giusberti, and J. Kriwet. 2022. A new cuspidate ptychodontid shark (Chondrichthyes; Elasmobranchii), from the Upper Cretaceous of Morocco with comments on tooth functionalities and replacement patterns. *Journal of African Earth Sciences* **187**:104440.

Amalfitano, J., L. Giusberti, E. Fornaciari, F. M. D. Vecchia, V. Luciani, J. Kriwet, and G. Carnevale. 2019. Large deadfalls of the "ginsu" shark *Cretoxyrhina mantelli* (Agassiz, 1835) (Neoselachii, Lamniformes) from the Upper Cretaceous of northeastern Italy. *Cretaceous Research* **98**:250–275.

Applegate, S. 1970. The vertebrate fauna of the Selma Formation of Alabama. *Fieldiana* (*Geology Memoirs*) **3**:433.

Bassett, D., K. G. Macleod, J. F. Miller, and R. L. Ethington. 2007. Oxygen isotopic composition of biogenic phosphate and the temperature of Early Ordovician seawater. *Palaios* **22**:98–103.

Bernal, D., and C. A. Sepulveda. 2005. Evidence for temperature elevation in the aerobic swimming musculature of the common thresher shark, *Alopias vulpinus*. *Copeia* **2005**:146–151.

Bernal, D., C. Sepulveda, and J. B. Graham. 2001. Water-tunnel studies of heat balance in swimming mako sharks. *Journal of Experimental Biology* **204**:4043–4054.

Bice, K. N., and K. Shimada. 2016. Fossil marine vertebrates from the Codell Sandstone Member (middle Turonian) of the Upper Cretaceous Carlile Shale in Jewell County, Kansas, USA. *Cretaceous Research* **65**:172–198.

Blanco-Piñón, A., L. M. Garibay–Romero, and J. Alvarado–Ortega. 2007. The oldest stratigraphic record of the Late Cretaceous shark *Ptychodus mortoni* Agassiz, from Vallecillo, Nuevo León, northeastern Mexico. *Revista Mexicana de Ciencias Geológicas* **24**:25–30.

Bonfil, R., M. Meÿer, M. C. Scholl, R. Johnson, S. O'Brien, H. Oosthuizen, S. Swanson, D. Kotze, and M. Paterson. 2005. Transoceanic migration, spatial dynamics, and population linkages of white sharks. *Science* **310**:100–103.

Bruner, J. C. 1998. Tooth replacement rates of *Carcharodon carcharias* (Linnaeus, 1758). P. 98 *in* AES 14th Annual Meeting, Program and Abstracts, Guelph, Ontario, Canada.

Cappetta, H. 1987. Chondrichthyes II: Mesozoic and Cenozoic Elasmobranchii. P. 193 *in Handbook of paleoichthyology*, Vol. 3B. Gustav Fischer, Jena, Germany.

Cappetta, H. 2012. Chondrichthyes: Mesozoic and Cenozoic Elasmobranchii: Teeth. P. 512 *in Handbook of paleoichthyology*, Vol. 3E. Pfeil, Munich.

Carey, F. G., and J. M. Teal. 1969. Mako and porbeagle: warm-bodied sharks. *Comparative Biochemistry and Physiology* **28**:199–204.

Carey, F. G., J. W. Kanwisher, O. Brazier, G. Gabrielson, J. G. Casey, and H. L. Pratt Jr. 1982. Temperature and activities of a white shark, *Carcharodon carcharias*. *Copeia* **1982**:254–260.

Carlson, J. K., K. J. Goldman, and C. G. Lowe. 2004. Metabolism, energetic demand, and endothermy. Pp. 203–224 *in Biology of sharks and their relatives*. CRC Press, Boca Raton, FL.

Case, G. R., and D. Baird. 1990. Selachians from the Niobrara Formation of the Upper Cretaceous (Coniacian) of Carrot River, Saskatchewan, Canda. *Canadian Journal of Earth Science* **27**:1084–1094.

Case, G. R., and D. R. Schwimmer. 1988. Late Cretaceous fish from the Blufftown Formation (Campanian) in western Georgia. *Journal of Paleontology* **62**:290–301.

Christie, C. H., and S. Nagihara. 2016. Geothermal gradients of the northern continental shelf of the Gulf of Mexico. *Geosphere* **12**:26–34.

https://doi.org/10.1017/pab.2024.45 Published online by Cambridge University Press

Ciampagalio, C. N., G. A. Wray, and B. H. Corliss. 2005. A toothy tale of evolution: convergence in tooth morphology among marine Mesozoic–Cenozoic sharks, reptiles, and mammals. *Sedimentary Record* **3**:4–8.

Ciampagalio, C. N., D. J. Cicimurri, J. A. Ebersole, and K. E. Runyon. 2013. A note on Late Cretaceous fish taxa recovered from stream gravels at site AGr-43 in Greene County, Alabama. *Alabama Museum of Natural History Bulletin* **31**(1):84–97.

Comans, C. M., S. M. Smart, E. R. Kast, Y. Lu, T. Lüdecke, J. N. Leichliter, D. M. Sigman, T. Ikejiri, and A. Martínez-García. 2024. Enameloid-bound $\delta^{15}N$ reveals large trophic separation among Late Cretaceous sharks in the northern Gulf of Mexico. *Geobiology* **22**:e12585.

Cooper, A. R., and S. Morris. 2004. Haemoglobin function and respiratory status of the Port Jackson shark, *Heterodontus portusjacksoni*, in response to lowered salinity. *Journal of Comparative Physiology B* **174**:223–236.

Cooper, J. A., C. Pimiento, H. G. Ferrón and M. J. Benton. 2020. Body dimensions of the extinct giant shark *Otodus megalodon*: a 2D reconstruction. *Scientific Reports* **10**:14596.

Cope, E. D. 1874. Review of the Vertebrata of the Cretaceous period found west of the Mississippi River. *Bulletin of the U. S. Geological and Geographical Survey of the Territories*. Department of Interior, Washington, D.C. P. 2303.

Coulson, A. B., M. J. Kohn, and R. E. Barrick. 2011. Isotopic evaluation of ocean circulation in the Late Cretaceous North American seaway. *Nature Geoscience* **4**:852–855.

Craig, H. 1966. Isotopic composition and origin of the Red Sea and Salton Sea geothermal brines. *Science* **154**:1544–1548.

Cumbaa, S. L., C. J. Underwood, and C. J. Schröder-Adams. 2013. Paleoenvironments and paleoecology of the vertebrate fauna from a Late Cretaceous marine bonebed, Canada. Pp. 509–524 *in* G. Arratia, H.-P. Schultze, and M. V. H. Wilson, eds. *Mesozoic fishes*. Vol. 5, *Global diversity and evolution*. Friedrich Pfeil, Munich, Germany.

Ehret, D. J., and T. L. Harrell Jr. 2018. Feeding traces on a pteranodon (Reptilia: Pterosauria) bone from the Late Cretaceous (Campanian) Mooreville Chalk in Alabama, USA. *Palaios* **33**:414–418.

Enax, J., O. Prymak, D. Raabe, and M. Epple. 2012. Structure, composition, and mechanical properties of shark teeth. *Journal of Structural Biology* **178**:290–299.

Everhart, M. J. 2004. Late Cretaceous interaction between predators and prey. Evidence of feeding by two species of shark on a mosasaur. *PalArch* **1**:1–7.

Ferrón, H. G. 2017. Regional endothermy as a trigger for gigantism in some extinct macropredatory sharks. *PLoS One* **12**:e0185185.

Fischer, J., S. Voigt, M. Franz, J. W. Schneider, M. M. Joachimski, M. Tichomirowa, J. Gotze, and H. Furrer. 2012. Palaeoenvironments of the late Triassic Rhaetian Sea: implications from oxygen and strontium isotopes of hybodont shark teeth. *Palaeogeography, Palaeoclimatology, Palaeoecology* **353–355**:60–72.

Fischer, J., J. W. Schneider, S. Voigt, M. M. Joachimski, M. Tichomirowa, T. Tütken, J. Gotze, and U. Berner. 2013. Oxygen and strontium isotopes from fossil shark teeth: environmental and ecological implications for Late Palaeozoic European basins. *Chemical Geology* **342**:44–62.

Forrest, J., E. Marcucci, and P. Scott. 2005. Geothermal gradients and subsurface temperatures in the northern Gulf of Mexico. *Gulf Coast Association of Geological Societies Transactions* **55**:233–248.

Fricke, H. C., B. Z. Foreman, and J. O. Sewall. 2010. Integrated climate model-oxygen isotope evidence for a North American monsoon during the Late Cretaceous. *Earth and Planetary Science Letters* **289**:11–21.

Gaube, P., C. D. Braun, G. L. Lawson, D. J. McGillicuddy, A. D. Penna, G. B. Skomal, C. Fischer, and S. R. Thorrold. 2018. Mesoscale eddies influence the movements of mature female white sharks in the Gulf Stream and Sargasso Sea. *Scientific Reports* **8**:7363.

Goldman, K. J. 1997. Regulation of body temperature in the white shark, *Carcharodon carcharias*. *Journal of Comparative Physiology B* **167**:423–429.

Gore, M. A., D. Rowat, J. Hall, F. R. Gell, and R. F. Ormond. 2008. Transatlantic migration and deep mid-ocean diving by basking shark. *Biology Letters* **4**:395–398.

Griffiths, M. L., R. A. Eagle, S. L. Kim, R. J. Flores, M. A. Becker, H. M. Maish IV, R. B. Traylor, *et al.* 2023. Endothermic physiology of extinct megatooth sharks. *Proceedings of the National Academy of Sciences USA* **210**:e2218153120.

Hamm, S. A., and K. Shimada. 2002. Associated tooth set of the Late Cretaceous lamniform shark, *Scapanorhynchus raphiodon* (Mitsukurinidae), from the Niobrara Chalk of Western Kansas. *Transactions of the Kansas Academy of Science* **105**:18–26.

Harrell, T. L., A. Perez-Huerta, and C. A. Suarez. 2016. Endothermic mosasaurs? Possible thermoregulation of Late Cretaceous mosasaurs (Reptilia, Squamata) indicated by stable oxygen isotopes in fossil bioapatite in comparison with coeval marine fish and pelagic seabirds. *Palaeontology* **59**:351–363.

Hättig, K., K. Stevens, D. Thies, G. Schweigert, and J. Mutterlose. 2019. Evaluation of shark tooth diagenesis-screening methods and the application of their stable oxygen isotope data for palaeoenvironmental reconstructions. *Journal of the Geological Society* **176**:482–491.

Heupel, M. R., and C. A. Simpfendorfer. 2008. Movement and distribution of young bull sharks *Carcharhinus leucas* in a variable estuarine environment. *Aquatic Biology* **1**:277–289.

Hoffman, B. L., S. A. Hageman, and G. D. Claycomb. 2016. Scanning electron microscope examination of the dental enameloid of the Cretaceous durophagous shark *Ptychodus* supports neoselachian classification. *Journal of Paleontology* **90**:741–762.

Hoyos-Padilla, E. M., A. P. Klimley, F. Galván-Magaña, and A. Antoniou. 2016. Contrasts in the movements and habitat use of juvenile and adult white sharks (*Carcharodon carcharias*) at Guadalupe Island, Mexico. *Animal Biotelemetry* **4**:14.

Ikejiri, T., J. A. Ebersole, H. L. Blewitt, and S. M. Ebersole. 2013. An overview of Late Cretaceous vertebrates of Alabama. *Alabama Museum of Natural History Bulletin* **31**(1):46–71.

Jambura, P. L., R. Kindlimann, F. Lopez-Romero, G. Marrama, C. Pfaff, S. Stumpf, J. Turtscher, C. J. Underwood, D. J. Ward, and J. Kriwet. 2019. Micro-computed tomography imaging reveals the development of a unique tooth mineralization pattern in mackerel sharks (Chondrichthyes; Lamniformes) in deep time. *Scientific Reports* **9**:9652.

Karnes, M. E., R. L. Chan, J. P. Kuntz, M. L. Griffiths, K. Shimada, M. A. Becker, H. M. Maisch, *et al.* 2024. Enigmatic carbonate isotope values in shark teeth: evidence for environmental and dietary controls. *Palaeogeography, Palaeoclimatology, Palaeoecology* **635**:111943.

Kast, E. R., M. L. Griffiths, S. L. Kim, Z. C. Rao, K. Shimada, M. A. Becker, H. M. Maish, *et al.* 2022. Cenozoic megatooth sharks occupied extremely high trophic positions. *Science Advances* **8**:eabl6529.

Kim, S. L., C. M. Del Rio, D. Casper, and P. L. Koch. 2012. Isotopic incorporation rates for shark tissues from a long-term captive feeding study. *Journal of Experimental Biology* **215**:2495–2500.

King, D. T., Jr. 1990. Upper Cretaceous marl-limestone sequences of Alabama: possible products of sea-level change, not climate forcing. *Geology* **18**:19–22.

King, D. T., Jr., and M. C. Skotnicki. 1994. Upper Cretaceous stratigraphy and sea-level history, Gulf Coastal Plain of central and eastern Alabama. *Geological Society of America Special Paper* **27**.

Kocsis, L., T. W. Vennemann, A. Ulianov, and J. M. Brunnschweiler. 2015. Characterizing the bull shark *Carcharhinus leucas* habitat in Fiji by the chemical and isotopic compositions of their teeth. *Environmental Biology of Fishes* **98**:1609–1622.

Kohn, M. J., and T. E. Cerling. 2002. Stable isotope compositions of biological apatite. *Reviews in Mineralogy and Geochemistry* **48**:455–488.

Kolodny, Y., and B. Luz. 1991. Oxygen isotopes in phosphates of fossil fish—Devonian to Recent. *Paleontological Society Special Publications* **6**:105–119.

Kolodny, Y., and M. Raab. 1988. Oxygen isotopes in phosphatic fish remains from Israel: paleothermometry of tropical Cretaceous and Tertiary shelf waters. *Palaeogeography, Palaeoclimatology, Palaeoecology* **64**:59–67.

Kolodny, Y., B. Luz, and O. Navon. 1983. Oxygen isotope variations in phosphate of biogenic apatites, I. Fish bone apatite—rechecking the rules of the game. *Earth and Planetary Science Letters* **64**:393–404.

Larocca Conte, G., A. Aleksinski, A. Liao, J. Kriwet, T. Mörs, R. B. Trayler, L. C. Ivany, M. Huber and S. L. Kim. 2024. Eocene shark teeth from peninsular Antarctica: windows to habitat use and paleoceanography. *Paleoceanography and Paleoclimatology* **39**:e2024PA004965.

https://doi.org/10.1017/pab.2024.45 Published online by Cambridge University Press

Lécuyer, C., R. Amiot, A. Touzeau, and J. Trotter. 2013. Calibration of the phosphate $\delta^{18}O$ thermometer with carbonate–water oxygen isotope fractionation equations. *Chemical Geology* **347**:217–226.

Leuzinger, L., L. Kocsis, J.-P. Billon-Bruyat, S. Spezzaferri, and T. W. Vennemann. 2015. Stable isotope study of a new chondrichthyan fauna (Kimmeridgian, Porrentruy, Swiss Jura): an unusual freshwater-influenced isotopic composition for the hybodont shark *Asteracanthus*. *Biogeosciences* **12**:6945–6954.

Leuzinger, L., L. Kocsis, Z. Luz, T. Vennemann, A. Ulyanov, and M. Fernández. 2023. Latest Maastrichtian middle- and high-latitude mosasaurs and fish isotopic composition: carbon source, thermoregulation strategy, and thermal latitudinal gradient. *Paleobiology* **49**:353–373.

Linnert, C., and J. Mutterlose. 2009. Evidence of increasing surface water oligotrophy during the Campanian–Maastrichtian boundary interval: calcareous nannofossils from DSDP Hole 390A (Blake Nose). *Marine Micropaleontology* **73**:26–36.

Liu, K. 2009. Oxygen and carbon isotope analysis of the Mooreville Chalk and late Santonian–early Campanian sea level and sea surface temperature changes, northeastern Gulf of Mexico, U.S.A. *Cretaceous Research* **30**:980–990.

Longinelli, A., and S. Nuti. 1973. Revised phosphate-water isotopic temperature scale. *Earth and Planetary Science Letters* **19**:373–376.

Mancini, E. A., and D. D. Soens. 1994. Paleoenvironments of the Tombigbee Sand Member of the Eutaw Formation (Upper Cretaceous) of Eastern Mississippi and Western Alabama. *Gulf Coast Association of Geological Societies Transactions* **44**:421–430.

Mancini, E. A., T. M. Puckett, and B. H. Tew. 1996. Integrated biostratigraphic and sequence stratigraphic framework for Upper Cretaceous strata of the eastern Gulf Coastal Plain, USA. *Cretaceous Research* **17**:645–669.

Mantell, G. A. 1839. *The wonders of geology; or, a familiar exposition of geological phenomena; being the substance of a course of lectures delivered at Brighton*. A.H. Maltby, New Haven, Conn.

McIntosh, A. P., K. Shimada, and M. J. Everhart. 2016. Late Cretaceous marine vertebrate fauna from the Fairport Chalk Member of the Carlile Shale in southern Ellis County, Kansas, U.S.A. *Transactions of the Kansas Academy of Science* **119**:222–230.

Mohr, R. C., T. S. Tobin, and E. M. Tompkins. 2024. Morphometric analysis of the Late Cretaceous *Placenticeras* of Alabama, USA: sexual dimorphism, allometry, and implications for taxonomy. *Paleobiology* **50**:239–270.

Morash, A. J., S. R. C. Mackellar, L. Tunnah, D. A. Barnett, K. M. Stehfest, J. M. Semmens, and S. Currie. 2016. Pass the salt: physiological consequences of ecologically relevant hyposmotic exposure in juvenile gummy sharks (*Mustelus antarcticus*) and school sharks (*Galeorhinus galeus*). *Conservation Physiology* **4**:cow036.

Moss, S. A. 1967. Tooth replacement in the lemon shark, *Negaprion brevirostris*. Pp. 319–329 *in* P. W. Gilbert, R. F. Matthewson and D. P. Rall, ed. *Sharks, skates, and rays*. Johns Hopkins Press, Baltimore, MD.

O'Neil, J. R., L. J. Roe, E. Reinhard, and R. E. Blake. 1994. A rapid and precise method of oxygen isotope analysis of biogenic phosphate. *Israel Journal of Earth Sciences* **43**:203–212.

Ostrom, P. H., S. A. Macko, M. H. Engel, J. A. Silfer, and D. Russell. 1990. Geochemical characterization of high molecular weight material isolated from Late Cretaceous fossils. *Organic Geochemistry* **16**:1139–1144.

Ostrom, P. H., S. A. Macko, M. H. Engel, and D. A. Russell. 1993. Assessment of trophic structure of Cretaceous communities based on stable nitrogen isotope analyses. *Geology* **21**:491.

Paladino, F. V., M. P. O'Connor, and J. R. Spotila. 1990. Metabolism of leatherback turtles, gigantothermy, and thermoregulation of dinosaurs. *Nature* **344**:858–860.

Parsons, G. R., G. W. Ingram, and R. Havard. 2002. First record of the goblin shark *Mitsukurina owstoni*, Jordan (Family Mitsukurinidae) in the Gulf of Mexico. *Southeastern Naturalist* **1**:189–192.

Peterson, S. V., C. R. Tabor, K. C. Lohmann, C. J. Poulsen, K. W. Meyer, S. J. Carpenter, J. M. Erickson, K. K. S. Matsunaga, S. Y. Smith, and N. D. Sheldon. 2016. Temperature and salinity of the Late Cretaceous Western Interior Seaway. *Geology* **44**:903–906.

Pimiento, C., J. L. Cantalapiedra, K. Shimada, D. J. Field, and J. B. Smaers. 2019. Evolutionary pathways toward gigantism in sharks and rays. *Evolution* **73**:588–599.

Poulsen, C. J., D. Pollard, and T. S. White. 2007. General circulation model simulation of the $\delta^{18}O$ content of continental precipitation in the middle Cretaceous: a model-proxy comparison. *Geology* **35**:199.

Pucéat, E., C. Lecuyer, S. M. F. Sheppard, G. Dromart, S. Reboulet, and P. Grandjean. 2003. Thermal evolution of Cretaceous Tethyan marine waters inferred from oxygen isotope composition of fish tooth enamels. *Paleoceanography and Paleoclimatology* **18**:1029.

Pucéat, E., C. Lécuyer, Y. Donnadieu, P. Naveau, H. Cappetta, G. Ramstein, B. T. Huber, and J. Kriwet. 2007. Fish tooth $\delta^{18}O$ revising Late Cretaceous meridional upper ocean water temperature gradients. *Geology* **35**:107.

Pucéat, E., M. M. Joachimski, A. Bouilloux, F. Monna, A. Bonin, S. Motreuil, P. Morinière, *et al.* 2010. Revised phosphate–water fractionation equation reassessing paleotemperatures derived from biogenic apatite. *Earth and Planetary Science Letters* **298**:135–142.

Puckett, T. M. 1991. Absolute paleobathymetry of Upper Cretaceous chalks based on ostracodes—evidence from the Demopolis Chalk (Campanian and Maastrichtian) of the northern Gulf Coastal Plain. *Geology* **19**:449.

Puckett, T. M. 1995. Planktonic foraminiferal and ostracode biostratigraphy of the late Santonian through early Maastrichtian strata in Dallas County, Alabama. *Geological Survey of Alabama Bulletin* **64**:1–59.

Raymond, D. E., W. E. Obsborne, C. W. Copeland, and T. L. Neathery. 1988. Alabama Stratigraphy. *Geological Survey of Alabama Circular* **140**:1–102.

R Core Team. 2022. *R: a language and environment for statistical computing*. R Foundation for Statistical Computing, Vienna, Austria. https://www.R-project.org.

Reif, W. E., D. McGill, and P. Motta. 1978. Tooth replacement rates of the sharks *Triakis semifasciata* and *Ginglymostoma cirratum*. *Zoologische Jahrbücher. Abteilung für Anatomie und Ontogenie de Tiere* **99**:151–156.

Roelofs, B., M. Barham, J. Cliff, M. Joachimski, L. Martin, and K. Trinajstic. 2017. Assessing the fidelity of marine vertebrate microfossil $\delta^{18}O$ signatures and their potential for palaeo-ecological and -climatic reconstructions. *Palaeogeography, Palaeoclimatology, Palaeoecology* **465**:79–92.

Roemer, C. F. 1849. *Texas: Mit besonderer Rücksicht auf deutsche Auswanderung und die physischen Verhältnisse des Landes. Mit einem naturwissenschaftlichen Anhange und einer topographisch-geognostischen Karte von Texas*. Bei Adolph Marcus, Bonn, Germany.

Schein, J. P., and R. D. Lewis. 2007. Actinopterygian fishes from Upper Cretaceous rocks in Alabama, with emphasis on the teleostean genus *Enchodus*. *Paludicola* **6**:41–86.

Schwimmer, D. R., G. D. Williams, J. L. Dobie, and W. G. Siesser. 1993. Late Cretaceous dinosaurs from the Blufftown Formation in western Georgia and eastern Alabama. *Journal of Paleontology* **67**:288–296.

Schwimmer, D. R., J. D. Stewart, and G. D. Williams. 1997. Scavenging by sharks of the genus *Squalicorax* in the Late Cretaceous of North America. *Palaios* **12**:71–83.

Shackleton, N. J., and J. P. Kennett. 1975. Laurentide ice sheet meltwater recorded in Gulf of Mexico deep-sea cores. *Science* **188**:147–150.

Shimada, K. 1997a. Paleoecological relationships of the Late Cretaceous lamniform shark, *Cretoxyrhina mantelli* (Agassiz). *Journal of Vertebrate Paleontology* **71**:926–933.

Shimada, K. 1997b. Skeletal anatomy of the Late Cretaceous lamniform shark, *Cretoxyrhina mantelli*, from the Niobrara Chalk in Kansas. *Journal of Vertebrate Paleontology* **17**:642–652.

Shimada, K. 2007. Skeletal and dental anatomy of lamniform shark, *Cretalamna appendiculata*, from Upper Cretaceous Niobrara Chalk of Kansas. *Journal of Vertebrate Paleontology* **27**:584–602.

Shimada, K. 2012. Dentition of Late Cretaceous shark, *Ptychodus mortoni* (Elasmobranchii, Ptychodontidae). *Journal of Vertebrate Paleontology* **32**:1271–1284.

Shimada, K., and D. D. Brereton. 2007. The Late Cretaceous lamniform shark, *Serratolamna serrata* (Agassiz) from the Mooreville Chalk of Alabama. *Paludicola* **6**:105–110.

Shimada, K., and D. J. Cicimurri. 2005. Skeletal anatomy of the Late Cretaceous shark, *Squalicorax* (Neoselachii: Anacoracidae). *Palaontologische Zeitschrift* **79**:241–261.

Shimada, K., and G. E. Hooks. 2004. Shark-bitten protostegid turtles from the Upper Cretaceous Mooreville Chalk, Alabama. *Journal of Paleontology* **78**:205–210.

https://doi.org/10.1017/pab.2024.45 Published online by Cambridge University Press

Shimada, K., C. K. Rigsby, and S. H. Kim. 2009. Partial skull of Late Cretaceous durophagous shark, *Ptychodus occidentalis* (Elasmobranchii: Ptychodontidae), from Nebraska, U.S.A. *Journal of Vertebrate Paleontology* **29**:336–349.

Shimada, K., M. J. Everhart, R. Decker, and P. D. Decker. 2010. A new skeletal remains of the durophagous shark, *Ptychodus mortoni*, from the Upper Cretaceous of North America: an indication of gigantic body size. *Cretaceous Research* **31**:249–254.

Shimada, K., M. A. Becker, and M. L. Griffiths. 2021. Body, jaw, and dentition lengths of macrophagous lamniform sharks, and body size evolution in Lamniformes with special reference to "off-the-scale" gigantism of the megatooth shark, *Otodus megalodon*. *Historical Biology* **33**:2543–2559.

Shipley, O. N., A. L. Newton, M. G. Frisk, G. A. Henkes, J. S. LaBelle, M. D. Camhi, M. W. Hyatt, H. Walters, and J. A. Olin. 2021. Telemetry-validated nitrogen stable isotope clocks identify ocean-to-estuarine habitat shifts in mobile organisms. *Methods in Ecology and Evolution* **12**:897–908.

Siverson, M. 1992. Biology, dental morphology and taxonomy of lamniform sharks from the Campanian of the Kristianstad Basin, Sweden. *Palaeontology* **35**:519–554.

Siverson, M., J. Lindgren, M. G. Newbrey, P. Cederstrom, and T. D. Cook. 2015. Cenomanian–Campanian (Late Cretaceous) mid-palaeolatitude sharks of *Cretalamna appendiculata* type. *Acta Palaeontologica Polonica* **60**:339–384.

Skotnicki, M. C., and D. T. King Jr. 1986. Depositional facies and sea-level dynamics of the Blufftown Formation, lower Campanian of east Alabama. *Southeastern Geology* **27**:53–67.

Smoothey, A. F., K. A. Lee, and V. M. Peddemors. 2019. Long-term patterns of abundance, residency, and movements of bull sharks (*Carcharhinus leucas*) in Sydney Harbour, Australia. *Scientific Reports* **9**:18864.

Szabo, M. W., W. E. Osborne, C. W. Copeland Jr., and T. L. Neathery. 1988. Geologic map of Alabama (1:250,000). Alabama Geological Survey Special Map 220. Geological Survey of Alabama, Tuscaloosa, Ala.

Tamburin, E., S. Kim, F. Elorriaga-Verplancken, D. Madigan, M. Hoyos-Padilla, A. Sánchez-González, A. Hernández-Herrera, J. Castillo-Geniz, C. Godinez-Padilla, and F. Galván-Magaña. 2019. Isotopic niche and resource sharing among young sharks (*Carcharodon carcharias* and *Isurus oxyrinchus*) in Baja California, Mexico. *Marine Ecology Progress Series* **613**:107–124.

Taylor, L. T., R. Totten, C. A. Suarez, L. A. Gonzalez, L. D. Martin, W. J. Lambert, D. J. Ehret, and T. L. Harrell. 2021. Oxygen isotopes from the teeth of Cretaceous marine lizards reveal their migration and consumption of freshwater in the Western Interior Seaway, North America. *Palaeogeography, Palaeoclimatology, Palaeoecology* **573**:e110406.

Tew, B. H. 2000. Depositional setting of the Arcola Limestone Member (Campanian) of the Mooreville Chalk, Eastern Gulf Plain. *Gulf Coast Association of Geological Societies Transactions* **50**:157–166.

Tütken, T., M. Weber, I. Zohar, H. Helmy, N. Bourgon, O. Lernau, K. P. Jochum, and G. Sisma-Ventura. 2020. Strontium and oxygen isotope analyses reveal Late Cretaceous shark teeth in Iron Age strata in the Southern Levant. *Frontiers in Ecology and Evolution* **8**:570032.

Vennemann, T. W., E. Hegner, G. Cliff, and G. W. Benz. 2001. Isotopic composition of recent shark teeth as a proxy for environmental conditions. *Geochimica et Cosmochimica Acta* **65**:1583–1599.

Vennemann, T. W., H. C. Fricke, R. E. Blake, J. R. O'Neil, and A. Colman. 2002. Oxygen isotope analysis of phosphates: a comparison of techniques for analysis of Ag_3PO_4. *Chemical Geology* **185**:321–336.

Vullo, R., E. Villalobos-Segura, M. Amadori, J. Kriwet, E. Frey, M. A. González González, J. M. Padilla Gutiérrez, C. Ifrim, E. S. Stinnesbeck, and W. Stinnesbeck. 2024. Exceptionally preserved shark fossils from Mexico elucidate the long-standing enigma of the Cretaceous elasmobranch *Ptychodus*. *Proceedings of the Royal Society B* **291**:20240262.

Watkins, D. K., and J. M. Self-Trail. 2005. Calcareous nannofossil evidence for the existence of the Gulf Stream during the late Maastrichtian. *Paleoceanography* **20**:2004PA001121.

Welton, B. J., and R. F. Farish. 1993. *The Collector's guide to fossil sharks and rays from the Cretaceous of Texas. Before Time*. Lewisville, Texas, Pp 204.

Woo, K., T. F. Anderson, L. B. Railsback, and P. A. Sandberg. 1992. Oxygen isotope evidence for high-salinity surface seawater in the Mid-Cretaceous Gulf of Mexico: implications for warm, saline deepwater formation. *Paleoceanography* **7**:673–685.

Zeichner, S. S., A. S. Colman, C. Polo-Silva, F. Galvan-Magana, and S. L. Kim. 2017. Discrimination factors and incorporation rates for organic matrix in shark teeth based on a captive feeding study. *Physiological and Biochemical Zoology* **90**:257–272.

Žigaitė, Ž., and M. Whitehouse. 2014. Stable oxygen isotopes of dental biomineral: differentiation at the intra- and inter-tissue level of modern shark teeth. *GFF* **136**:337–340.

https://doi.org/10.1017/pab.2024.45 Published online by Cambridge University Press